

Electronic Supporting Information for

Single Particle Level Insights into Photoactivation
and Suppression of Auger Recombination in
Aqueous Cu-Doped CdS Quantum Dots

*Sharmistha Das, Gourab Rana, Fariyad Ali, Anindya Datta**

Department of Chemistry
Indian Institute of Technology Bombay
Mumbai 400076, India

e-mail: anindya@chem.iitb.ac.in (AD) Phone: +91 22 2576 7149, Fax: +91 22 2576 7152

Table of Contents

Sr. No.	Content	Description	Page
1.	Note SN1	Calculation of dopant concentration in Cu:CdS quantum dots	S3
2.	Table ST1	Cu:Cd and Cd:S ratios as determined from ICP-AES	S3
3.	Figure S1	XPS Spectra	S4
4.	Figure S2	Second Derivative of Absorption Spectrum	S4
5.	Table ST2	QD size calculation	S5
6.	Figure S3	QD size variation with reaction time	S6
7.	Figure S4	Variation of UV-Vis absorption with reaction time	S7
8.	Figure S5	Excitation wavelength dependent PL Spectra	S7
9.	Table ST3	Calculated Photoluminescence Quantum Yield	S7
10.	Figure S6	Effect of doping level on PL spectra and color	S8
11.	Figure S7	MLC _{CBT} band in UV-Vis absorbance	S8
12.	Figure S8	Variation of PLQY with increasing reaction time	S9
13.	Table ST4	Temporal parameters for PL of undoped and Cu:CdS QDs	S10
14.	Figure S9	Wavelength dependent nanosecond PL transients	S10
15.	Table ST5	FCS parameters for undoped and Cu:CdS QDs.	S11
16.	Figure S10	Power dependence of FCS curves	S11
17.	Table ST6	Variation of FCS fitting parameters with increasing excitation power	S12
18.	Figure S11	FCS control experiment with dye C102	S13
19.	Figure S12	Variation of PL intensity and Diffusion time with excitation power	S13

Note SN1: Calculation of dopant concentration in Cu:CdS quantum dots.

The mole fractions of Cd, Cu and S in the system was determined by Inductively coupled plasma atomic emission spectra (ICP-AES) is performed on an ARCOS simultaneous ICP spectrometer (SPECTRO Analytical Instruments GmbH, Germany) equipped with a CCD detector of wavelength range 130–770 nm and a resolution of 9 pm. A sample aliquot was first digested with aqua-regia and then analysed. The results are as follows:

Table ST1: Cu:Cd and Cd:S ratios as determined from ICP-AES measurements.

S. No.	Precursor Ratio added for synthesis (Cu:Cd:S)	Cu:Cd (%Cu)	Cd:S	Number of Cu atoms per QD
1	0:1:1.8	0	1.70	0
2	0.005:1:1.8	0.00197 (0.2%)	1.66	0.74
3	0.01:1:1.8	0.00297 (0.3%)	1.65	1.12
4	0.02:1:1.8	0.00675 (0.67%)	1.65	2.55

Calculation of number of Cu-atoms per CdS quantum dots from ICP-AES results.

Diameter of Cu:CdS QDs = 3.3 nm;

Density of CdS (d) = 4.82 g cm⁻³; Molar Mass (M_{CdS}) = 144.46 g mol⁻¹

Radius of QDs (R) = 1.65 nm = 1.65×10⁻⁷ cm

Volume of QDs (V) = $\frac{4}{3}\pi R^3 = 1.881 \times 10^{-20}$ cm³

Mass of CdS (M) = $d \times V = 4.82 \text{ g cm}^{-3} \times 1.881 \times 10^{-20} \text{ cm}^3 = 9.065 \times 10^{-20}$ g

Moles of CdS (m) = $\frac{M}{M_{CdS}} = \frac{9.065 \times 10^{-20} \text{ g}}{144.46 \text{ g mol}^{-1}} = 0.063 \times 10^{-20}$ moles

No of moles of Cd = No of moles of CdS

No of Cd atoms = $m \times N_A = 0.063 \times 10^{-20} \text{ mol} \times 6.023 \times 10^{23} \text{ mol}^{-1}$
 = 377.95 Cd atoms per QD

Cu:Cd Ratio = 0.00197

No of Cu atoms per QD = 0.00197 × 377.95 = 0.744 atoms per QD

Similarly the calculation was done for other samples as well and the results are summarized in Table ST1.

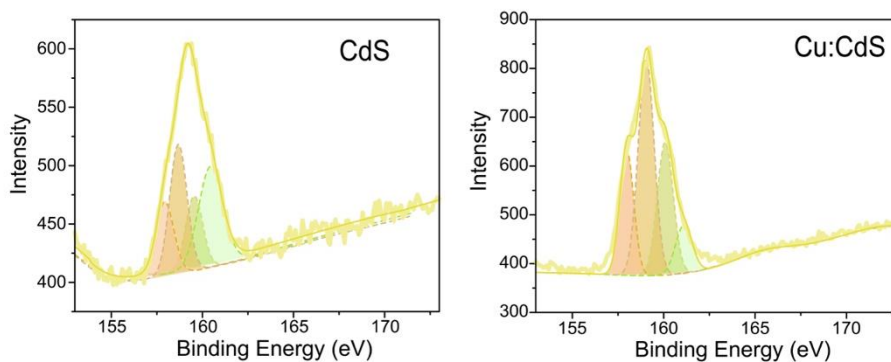


Figure S1. XPS Spectra. High resolution XPS spectra of S 2p region for (A) CdS QDs and (B) Cu:CdS QDs (0.3%).

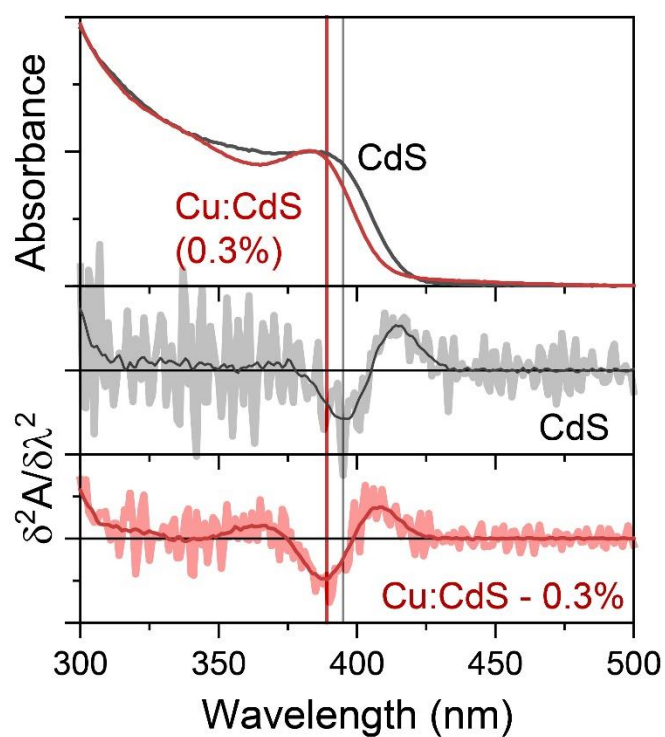


Figure S2. Second Derivative of Absorption Spectrum. (A) Absorption spectra of CdS QDs and Cu:CdS QDs (0.3%) and their corresponding second derivative spectra. The absorption onset is indicated with an arrow.

Table ST2. QD size calculation. Experimental QD size (TEM imaging) and calculated size (using Brus equation).

Size	CdS	Cu:CdS (0.3%)
Calculated	3.98	3.71
Experimental	3.6	3.3

$$\Delta E(r) = E_{gap} + \frac{h^2}{8r^2} \left(\frac{1}{m_e^*} + \frac{1}{m_h^*} \right)$$

E_{gap} = bulk band gap (2.41 eV for CdS); $m_e^* = 0.2m_e$ and $m_h^* = 0.8m_e$ for CdS

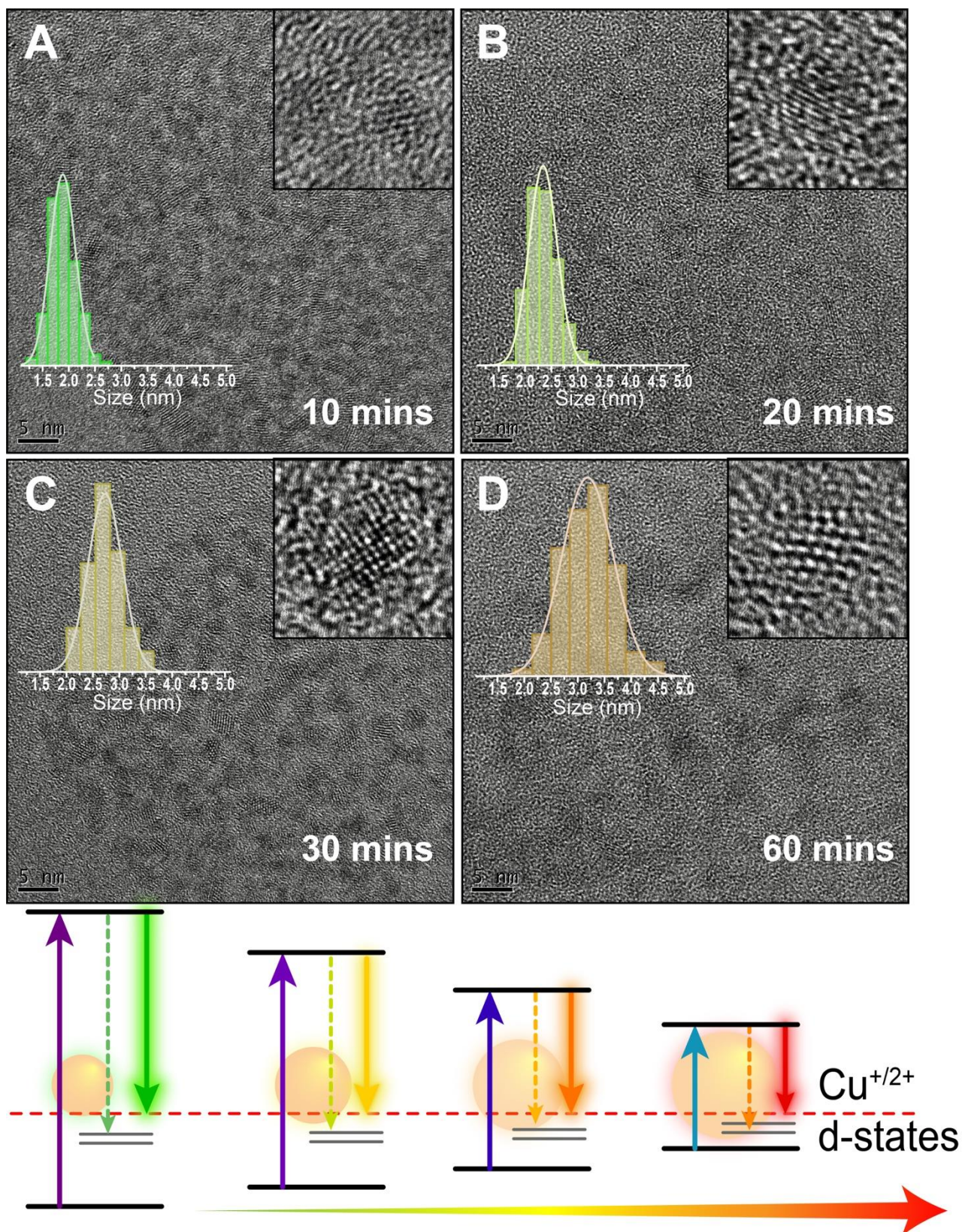


Figure S3. QD size variation with reaction time. TEM images of CdS quantum dot samples extracted at various reaction times and corresponding size distributions. Bottom panel depicts a schematic representation of the origin of color tunability in the samples due to variation of size and bandgap of QDs with increasing reaction time.

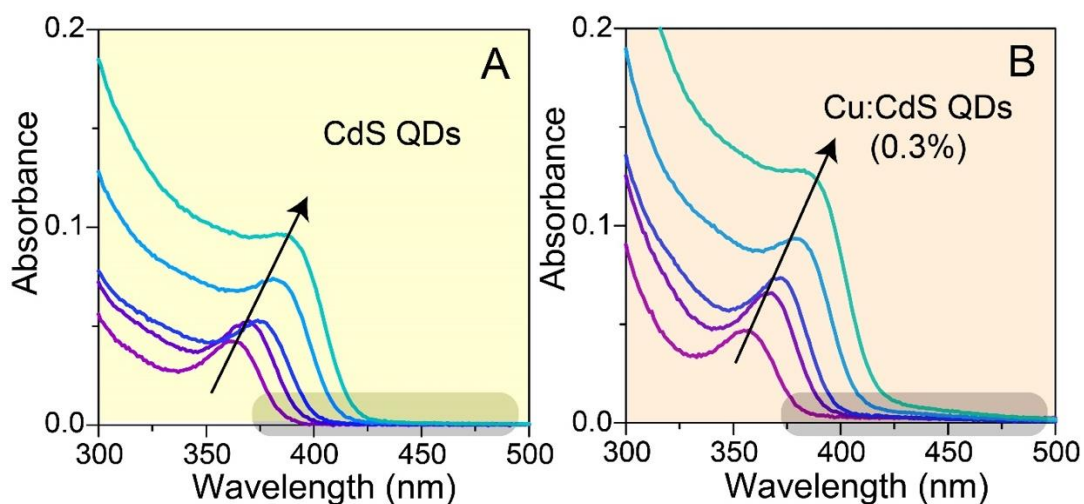


Figure S4. Variation of UV-Vis absorption with reaction time. Absorption spectra of sample aliquots taken with increasing reaction time for A) CdS QDs and B) 0.3% Cu:CdS QDs. The absorbance value increases as the reaction progresses indicating growth of the nanocrystals.

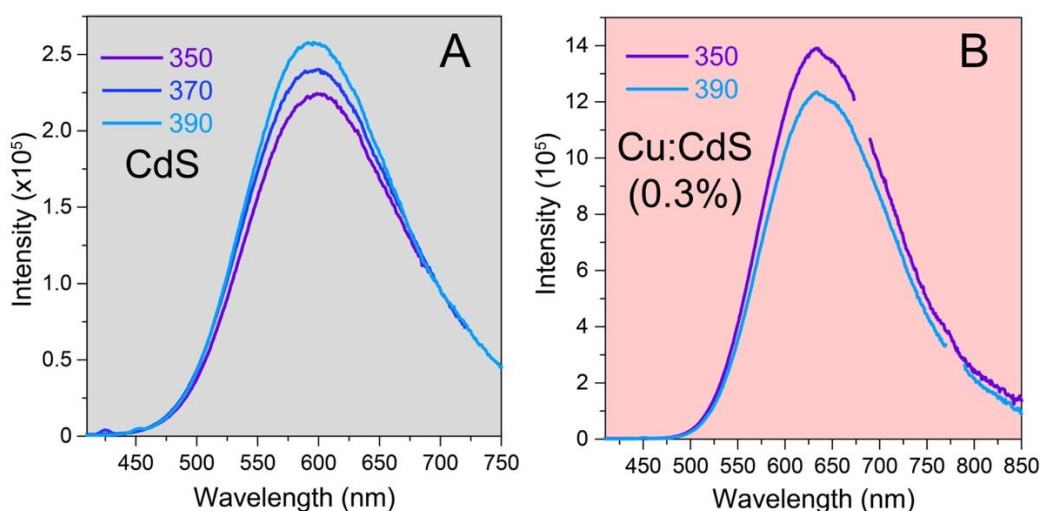


Figure S5. Excitation wavelength dependent PL Spectra. PL spectra of A) CdS QDs and B) 0.3% Cu:CdS QDs with varying excitation wavelength as indicated.

Table ST3. Photoluminescence Quantum Yields. Photoluminescence QY values of Cu:CdS QD samples after 60 min reaction time.

Sample	QY
CdS	0.05
Cu-0.5%	0.28
Cu-1.0%	0.32
Cu-2.0%	0.25

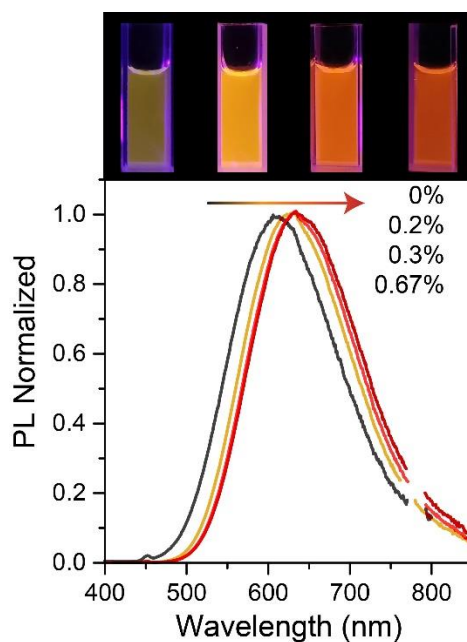


Figure S6. Effect of doping level on PL spectra and color. Variation of PL color and PL spectral change ($\lambda_{ex} = 380$ nm) with increasing dopant concentration after 90 minutes reaction. While there is no significant shift in PL maxima as Cu% increases from 0.2% to 0.67%, however the spectra broadens towards the red-wavelength region.

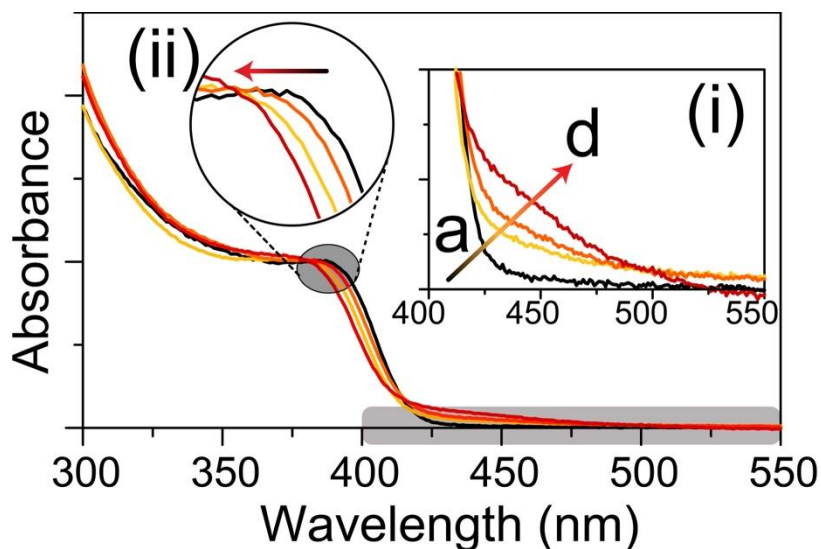


Figure S7. MLC_{CB}T band in UV-Vis absorbance. Normalized absorption spectra a) CdS QDs and Cu-doped QDs with %Cu c) 0.2%, d) 0.3%, and d) 0.67%. *Inset of D:* (i) Magnified view of the tail end of the absorption spectra showing the MLC_{CB}CT transition. (ii) Magnified view showing the gradual blue shift of absorption peak with increase in dopant concentration.

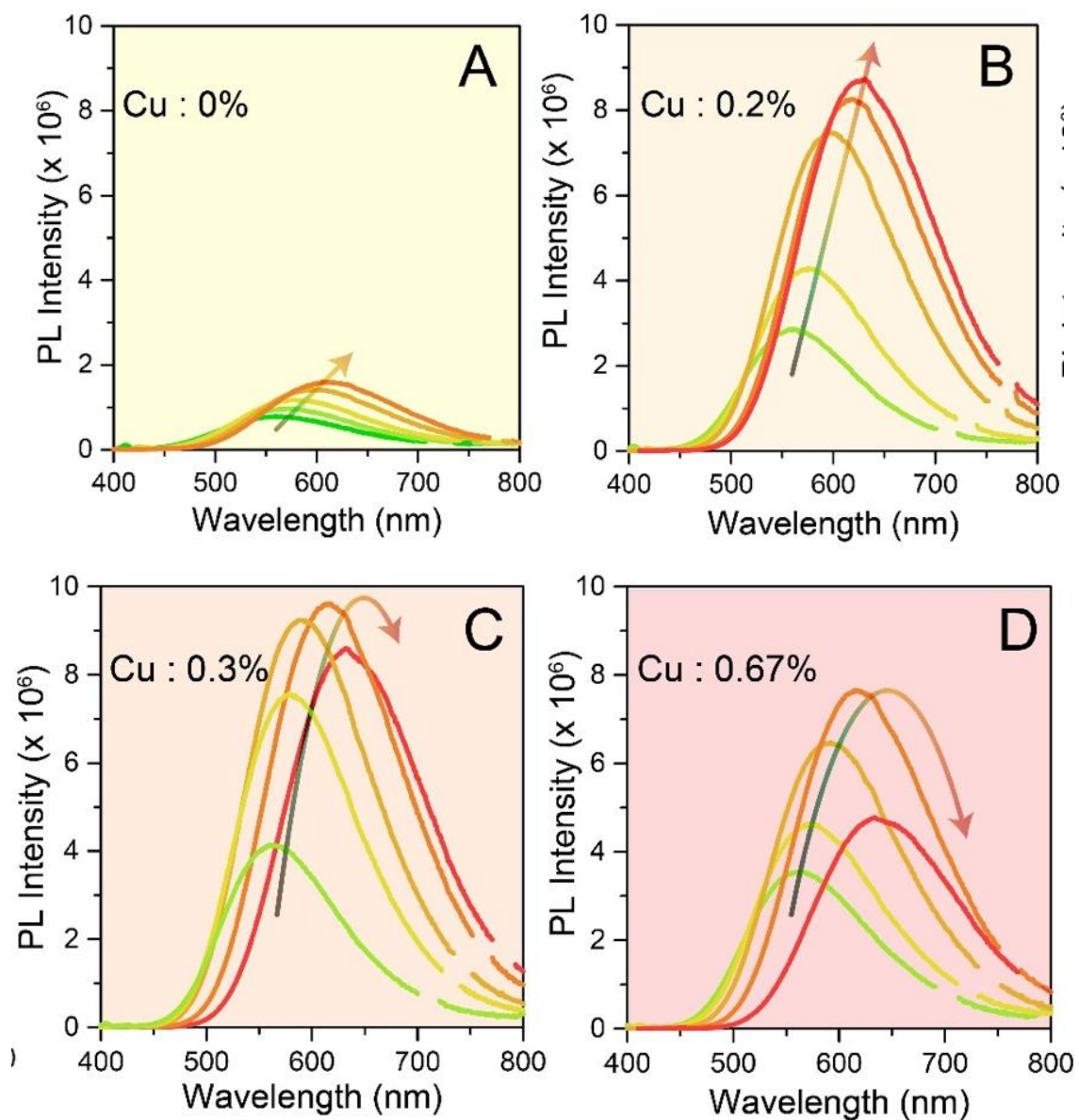


Figure S8. Variation of PLQY with increasing reaction time for a) CdS QDs and Cu-doped CdS QDs with Cu: Cd concentration of (B) 0.2%, (C) 0.3% and (D) 0.67%.

Table ST4. Temporal parameters for PL of undoped and Cu-doped CdS QDs

Sample	a_1 ($\tau_1 = 1.2$ ns)	a_2 ($\tau_2 = 16$ ns)	a_3 ($\tau_3 = 94$ ns)	a_4 ($\tau_4 = 530$ ns)
CdS	0.76	0.11	0.13	-
0.2% Cu:CdS	0.41	0.11	0.07	0.41
0.3% Cu:Cds	0.32	0.11	0.05	0.52
0.67% Cu:CdS	0.29	0.11	0.04	0.56

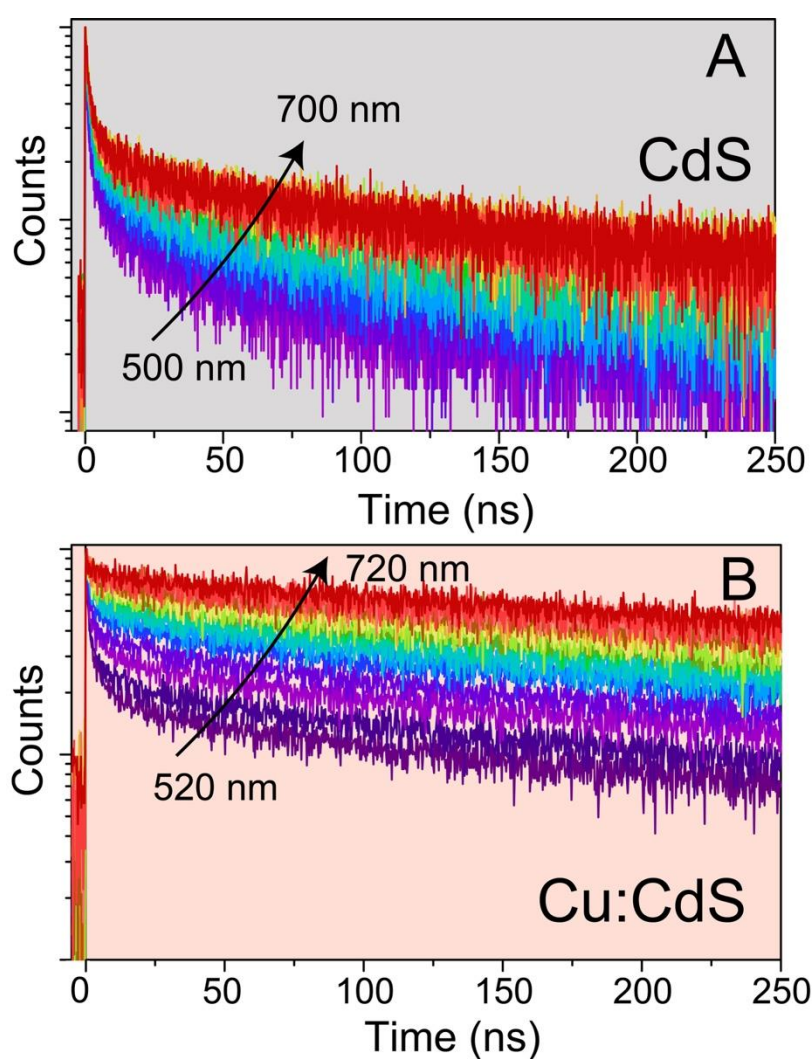


Figure S9. Wavelength dependent nanosecond PL transients. Wavelength dependent PL transients of (A) undoped CdS QDs and (B) 0.3% Cu:CdS QDs ($\lambda_{ex} = 380$ nm).

Table ST5. FCS parameters for undoped and Cu:CdS QDs. Parameters off-state fraction (T), Blinking Time (τ_T), stretching exponent (β), number of molecules N and counts per molecule (cpm) as obtained from fitting of PL correlation curves of recorded with 3 μ W excitation power.

Sample	T	τ_T (μ s)	β	Counts per molecule	$\langle N \rangle$
CdS	0.67 ± 0.057	120 ± 11	0.57 ± 0.07	425 ± 49	7.55 ± 0.82
Cu-0.2%	0.36 ± 0.008	103 ± 11	0.75 ± 0.079	911 ± 89	11.4 ± 1.1
Cu-0.3%	0.29 ± 0.012	87 ± 9	0.87 ± 0.073	1422 ± 149	14.5 ± 0.99
Cu-0.67%	0.5 ± 0.03	115 ± 10	0.69 ± 0.054	838 ± 92	10.2 ± 1.2

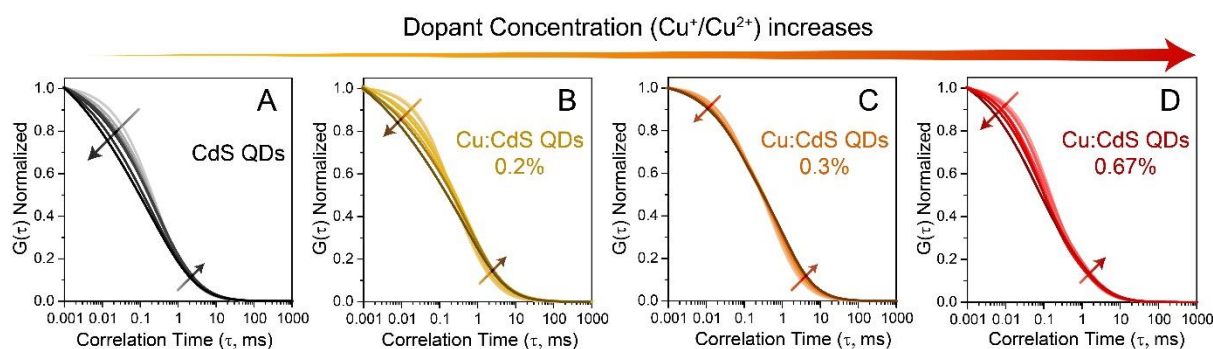


Figure S10. Power dependence of FCS curves. Normalized fluorescence correlation fitting curves at various excitation power depicting the change in line shape of the correlation curves with increasing excitation power for A) CdS QDs, and Cu:CdS QDs with Cu% (B) 0.2%, (C) 0.3% and (D) 0.67%.

Table ST6. Variation of FCS fitting parameters with increasing excitation power. Parameters off-state fraction (T), Blinking Time (τ_T) and stretching exponent (β) as obtained from fitting of PL correlation curves recorded at various excitation powers.

Exc. Power (μW)	T	τ_T (μs)	β
CdS QDs			
2.9	0.67 ± 0.057	120 ± 11	0.57 ± 0.07
5.8	0.68 ± 0.07	86 ± 8	0.53 ± 0.065
10.2	0.71 ± 0.068	68 ± 5	0.48 ± 0.052
14.5	0.73 ± 0.09	61 ± 7	0.46 ± 0.058
18.8	0.74 ± 0.008	54 ± 6	0.39 ± 0.048
23.2	0.75 ± 0.11	50 ± 4	0.29 ± 0.036
29	0.76 ± 0.04	47 ± 5	0.25 ± 0.028
Cu:CdS QDs (0.2%)			
2.9	0.36 ± 0.008	103 ± 11	0.75 ± 0.079
5.8	0.39 ± 0.04	89 ± 10	0.65 ± 0.052
10.2	0.52 ± 0.06	79 ± 9	0.48 ± 0.041
14.5	0.70 ± 0.065	68 ± 6	0.38 ± 0.035
18.8	0.74 ± 0.08	59 ± 4	0.42 ± 0.031
23.2	0.76 ± 0.12	47 ± 5	0.34 ± 0.033
29	0.79 ± 0.09	41 ± 4	0.32 ± 0.031

Exc. Power (μW)	T	τ_T (μs)	β
Cu:CdS QDs (0.3%)			
2.9	0.29 ± 0.012	87 ± 9	0.87 ± 0.073
5.8	0.35 ± 0.009	81 ± 10	0.77 ± 0.068
10.2	0.39 ± 0.03	75 ± 6	0.69 ± 0.048
14.5	0.40 ± 0.05	68 ± 8	0.65 ± 0.057
18.8	0.41 ± 0.061	62 ± 6	0.61 ± 0.037
23.2	0.43 ± 0.04	59 ± 5	0.57 ± 0.022
29	0.46 ± 0.057	51 ± 4	0.50 ± 0.031
Cu:CdS QDs (0.67%)			
2.9	0.5 ± 0.03	115 ± 10	0.69 ± 0.054
5.8	0.52 ± 0.025	103 ± 12	0.65 ± 0.061
10.2	0.57 ± 0.06	89 ± 7	0.62 ± 0.058
14.5	0.61 ± 0.073	73 ± 8	0.61 ± 0.042
18.8	0.64 ± 0.08	67 ± 8	0.57 ± 0.035
23.2	0.67 ± 0.055	57 ± 5	0.49 ± 0.043
29	0.69 ± 0.091	42 ± 4	0.41 ± 0.031

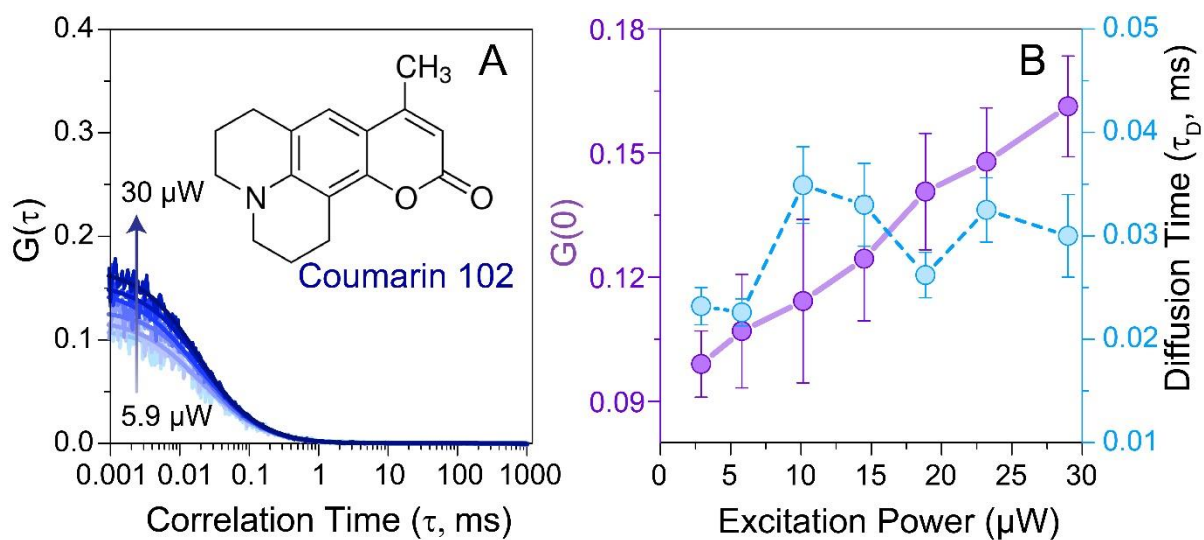


Figure S11. FCS control experiment with dye C102. (A) Fluorescence correlation curves of C102 in water with increasing excitation power. (B) Variation of initial correlation amplitude $G(0)$ and diffusion time (τ_D) as a function of excitation power. Slight increase in initial correlation amplitude with increasing excitation power arises from photobleaching effect.

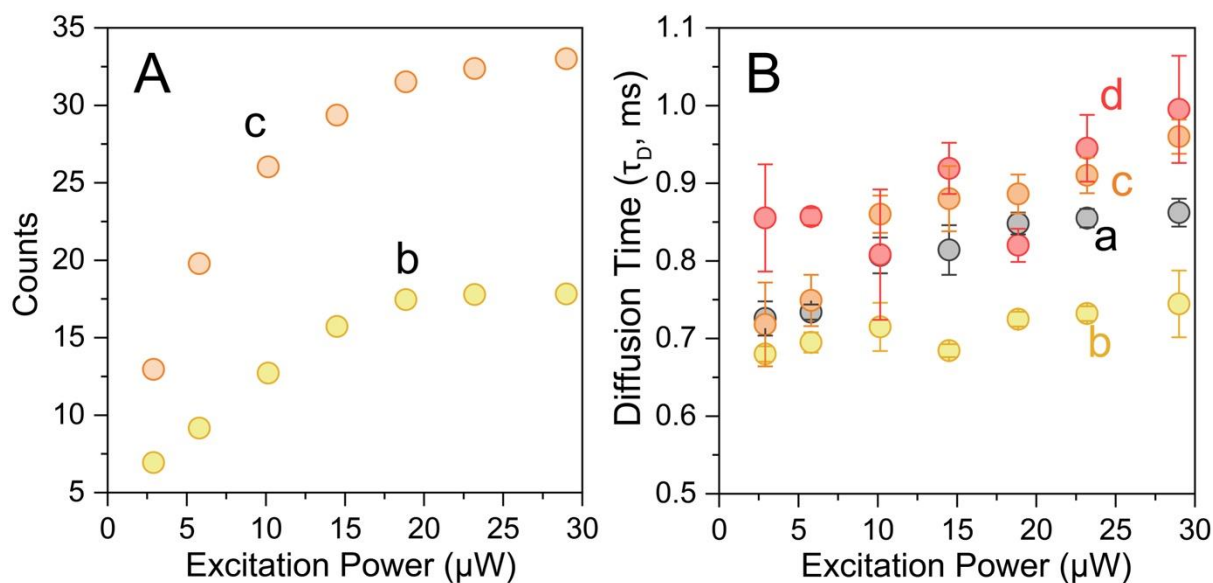


Figure S12. Variation of (A) PL intensity and (B) Diffusion time τ_D with increasing excitation power for a) CdS QDs and Cu:CdS QDs with Cu% as b) 0.2%, b) 0.3% and d) 0.67%.